

## Comb-shaped polymers to enhance hydroxide transport in anion exchange membranes†

Nanwen Li,<sup>\*a</sup> Tingzi Yan,<sup>b</sup> Zheng Li,<sup>a</sup> Thomas Thurn-Albrecht<sup>b</sup> and Wolfgang H. Binder<sup>\*a</sup>

Received 21st January 2012, Accepted 24th May 2012

DOI: 10.1039/c2ee22050d

**Comb-shaped poly(2,6-dimethyl-1,4-phenylene oxide) (PPO) polymers with quaternary ammonium (QA) groups have been synthesized organizing into well-defined micro-morphology for efficient anion (hydroxide) transport. These molecular comb structures show a dramatic enhancement in conductivity and water resistance compared with non-comb-shaped PPOs.**

There is technological interest in materials with high ionic conductivity, both in biological contexts and in the field of energy-related materials.<sup>1,2</sup> Ion exchange membranes, for example, have been studied widely for application in many fields,<sup>3–7</sup> the purification of pharmaceuticals, production of salt from seawater, wastewater treatment, and electrochemical devices (*i.e.*, acidic/alkaline fuel cells, batteries, electrodialysis, electrolysis and electrodeionization). Among them, the alkaline fuel cell (AFC) is considered to be a more promising energy conversion device for stationary and mobile applications compared with the acidic fuel cell because of its significant advantage

of improved oxygen reduction kinetics and better fuel oxidation kinetics, which can lead to higher efficiencies and enable the use of non-precious metal catalysts, greatly reducing the cost of the device.<sup>8–11</sup>

The anion (hydroxide, OH<sup>−</sup>) exchange membrane (AEM), which is one of the key components of AFCs, provides two major functions – selective ion transport (conductor) and electric insulation (separator) between two electrodes. An ideal membrane should possess a stable matrix and continuous ionic channels across the membrane with good ion mobility, while maintaining its structural integrity and stability under particular (alkaline and aqueous) conditions. Low conductivity was often observed for AEMs when compared to acidic proton exchange membranes (PEMs) due to the inherently lower mobility of hydroxyl ions and the weak basicity of the cation site.<sup>12,13</sup> Basically, the ionic conductivity is directly related to a combination of the ion exchange capacity (IEC), the ion mobility, its hydration level, and its micro-morphology.<sup>14–16</sup> Thus, the major difference in conductivity between PEMs and AEMs is rationalized by considering the mobility or dissociation of ions (H<sup>+</sup> or OH<sup>−</sup>). For instance, the ion mobility of H<sup>+</sup> is 4.76, whereas the OH<sup>−</sup> is only 2.69 relative to K<sup>+</sup> in infinitely dilute solution at 298 K (K<sup>+</sup> = 1).<sup>15,16</sup> Moreover, the sulfonic acids were considered strong acids in PEM (the pK<sub>a</sub> of aryl sulfonic acid has been estimated to be on the order of −1),<sup>17</sup> while the quaternary ammoniums were weak bases with a pK<sub>b</sub> on the order of 4. Therefore, dissociation of the quaternary ammonium ions presents a considerable theoretical barrier for efficient hydroxide conduction in an AEM. A variety of AEMs based upon pre-existing polymer systems have also been described in the recent literature, displaying

<sup>a</sup>Institute of Chemistry, Chair of Macromolecular Chemistry, Division of Technical and Macromolecular Chemistry, Faculty of Natural Sciences II (Chemistry, Physics and Mathematics), Martin-Luther-University Halle-Wittenberg, Halle 06120, Germany. E-mail: linanwen@gmail.com; wolfgang.binder@chemie.uni-halle.de

<sup>b</sup>Institute of Physics, Faculty of Natural Sciences II (Chemistry, Physics and Mathematics), Martin-Luther-University Halle-Wittenberg, Halle D-06120, Germany

† Electronic supplementary information (ESI) available: The synthesis and characterization of PPO-DMHDA-*x* and PPO-TMA membranes. See DOI: 10.1039/c2ee22050d

### Broader context

The search for new highly conducting anion exchange membranes (AEMs) has been a subject of intense research because of their potential applications in alkaline fuel cells (AFCs). Comb-shaped copolymers with quaternized poly(2,6-dimethyl phenylene oxide) (PPO) backbones and grafting alkyl chains displaying nanophase-separated morphology were designed and prepared. The unique polymer architecture results in nanophase separation between the conducting (quaternized PPO) and non-conducting domains (grafting alkyl chains), which shows an interconnected hydrophilic network of small ionic clusters of 5–10 nm in size, and thus gives rise to high anion conductivities. Comb-shaped membranes with low water uptake (10–20 wt%) have higher hydroxide conductivity values than those of non-comb-shaped membranes. High conductivities and excellent alkaline stability, coupled with low water uptake and dimensional swelling, suggest that the comb-shaped architecture is a promising approach for the design of AEMs to be used in alkaline fuel cells for automotive applications with low-pollution and high energy efficiency, in which fast electrode kinetics and non-precious electrocatalysts may be present.

a wide range of conductivities.<sup>18–24</sup> Mostly, a high hydroxide conductivity could only be achieved in those materials having a high ionic content and water uptake, which in turn would generally suffer from significant swelling in water and thus loss of the mechanical properties. Zhang *et al.*<sup>25</sup> have successfully introduced the strong organic base of guanidine into poly(arylene ether sulfone) for the enhancement of hydroxide-ion conductivity. The resulting membranes still showed improved hydroxide conductivity but only due to high water uptake. Park and co-workers<sup>26,27</sup> reported that AEMs aminated by an amination agent with long alkyl chains (six carbon atoms) showed higher water uptake and thus better hydroxide conductivity than AEMs based on trimethylamine. More recently, sequenced hydrophilic and hydrophobic groups as block copolymers were claimed to be effective for this purpose.<sup>28,29</sup> However, research on this class of copolymers is still in the initial stages, and the precise control of nanoscale morphology of multi-block copolymers is often restricted due to the polydispersity of each block.<sup>30</sup> Therefore, increasing the ionic conductivity of AEMs to achieve higher operation efficiencies remains a significant challenge and is currently an area of intense research.

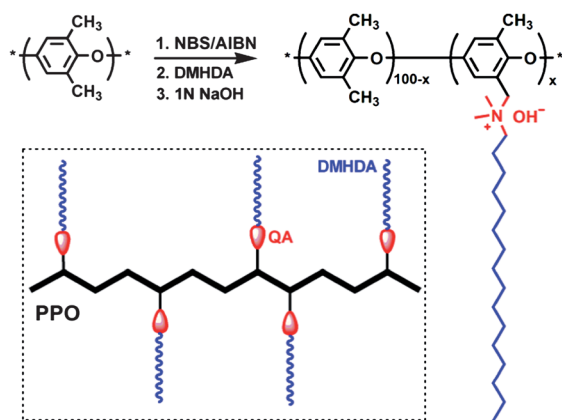
In order to fully understand and enhance the role of AEMs it is necessary to study materials with controlled polymer structure, ion exchange capacity (IEC) and microphase separated morphological structure. However, it is difficult to independently control both the polymer membrane's morphology and the IEC in a systematic manner. In an effort to exert more control over these parameters, we devised a method to synthesize comb-shaped, hydroxide-conducting copolymers with a hydrophobic grafting chain and a functionalized polymer backbone with quaternary ammonium (QA) groups, as shown in Scheme 1. Herein, the poly(phenylene oxide) (PPO) was chosen as polymer backbone because of its commercial availability as well as its high thermal, mechanical and chemical stabilities.<sup>31</sup>

Brominated poly(phenylene oxide) (Br-PPO) could be synthesized readily by bromination of the methyl-groups of commercially available PPO ( $M_n = 20\,000$ ,  $M_w/M_n = 1.5$ ). Usually, the bromination can take place either at the benzylic position or at the aromatic rings, depending on the reagents and reaction conditions.<sup>32,33</sup> In the present work, the bromination reaction occurs exclusively at the benzylic position of PPO using *N*-bromosuccinimide (NBS) and azobisisobutyronitrile (AIBN) at 135 °C in a refluxing chlorobenzene solution. The <sup>1</sup>H NMR analysis (Fig. S1†) indicated that partially methyl-

brominated PPOs were obtained with excellent selectivity at high yields without phenyl-brominated or methyl-dibrominated derivatives in a short reaction time (3 h). The bromination yields (which were calculated from the molar amount of NBS introduced into the reaction and the amount of bromine detected in the brominated PPO) were in the range of 70–85% (Table S1†). Thus, the degree of substitution ( $x$  value) ranged from 20 to 55.

Synthesis of the comb-shaped ionomers PPO-DMHDA- $x$  was achieved by the Menshutkin reaction with *N,N*-dimethyl-1-hexadecylamine (DMHDA), and subsequent hydroxide exchange. The experimental IEC values (Table S1†) of PPO-DMHDA- $x$  were determined as ranging from 1.08 to 1.92 meq. g<sup>-1</sup> by acid–base titration, and are similar to the values from <sup>1</sup>H NMR results. The PPO-DMHDA- $x$  exhibits excellent solubility in pure acetone, methanol, *n*-propanol and chloroform (Table S3†). However, it is insoluble in pure water, even at 80 °C, suggesting that it can be used in the catalyst layer without loss arising from solubility. Separate thermogravimetric analyses (TGA) were conducted to verify the stability of all membranes reported in this study. The decomposition temperature of QA groups (see Fig. S4†) was up to 140 °C. The value is similar to the reported AEMs based on trimethylamine.<sup>24,25</sup> Details of the synthesis and polymer characterization are available in the ESI†.

We hypothesized that the hydrophilic polymer main chain (PPO) is immiscible with the hydrophobic aliphatic grafting chain, thus driving comb-shaped PPOs to self-assemble and form nanoscale domains containing quaternary ammonium-ions, which in turn might facilitate hydroxide transport. To test this hypothesis, the nanostructure of the comb-shaped PPOs was characterized using small-angle X-ray scattering (SAXS). A conventional AEM based on PPO and trimethylamine, which was prepared according to previous reports<sup>32,33</sup> (PPO-TMA-20, IEC = 1.39 meq. g<sup>-1</sup>), was included for comparison. Fig. 1(a) shows the corresponding SAXS profiles, which show a clear peak for all comb-shaped PPOs, but not for the PPO-TMA-20 sample. This result is indicative of a nanophase separation between the hydrophilic main chain including the quaternary ammonium-ions and the hydrophobic aliphatic side chains leading to a periodic structure at a length scale  $d = 2\pi/q_{\max}$ , where  $q_{\max}$  is the peak position.<sup>34–36</sup> The corresponding values fall into the range of 1.79–2.13 nm<sup>-1</sup> ( $d = 2.95$ – $3.51$  nm), which roughly corresponds to the length of the aliphatic side chains. Accordingly the periodicity



**Scheme 1** Synthesis of comb-shaped polymers PPO-DMHDA- $x$  containing quaternary ammonium (QA) groups.

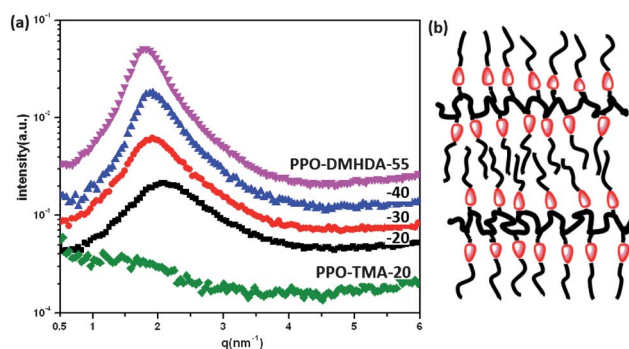


**Fig. 1** (a) Small angle X-ray scattering (SAXS) of comb-shaped PPO and PPO-TMA-20 membranes in the dry state. Individual datasets are shifted in the  $y$  direction. (b) Schematic depiction of comb-shaped PPO forming a lamellar microstructure.

$d$  increases with increasing content of DMHDA. This result is consistent with lamellar microstructures as suggested by the comb-shaped architecture. The large width of the peaks indicates that the arrangement of the phase separated domains is only locally correlated, and no long-range ordered structures are formed. Interestingly the peak width decreases with increasing substitution (see ESI†). The fact that no second order peak is visible might indicate a weak separation between the two components. As will be shown below the self-assembled structure visible in the SAXS experiments had a strong influence on water uptake and ionic transport.

We then performed AFM observations for the PPO-DMHDA-20 membrane. As shown in Fig. 2, the dark areas represent hydrophilic (ionic) domains, and the brighter areas represent hydrophobic domains. The phase surface image exhibits clear hydrophilic–hydrophobic phase separation with an interconnected hydrophilic network of small ionic domains with size of 5–10 nm, which is the result of the comb-shaped structure. In addition, ionic domains measuring several tens of nanometers, spreading as a cloudlike belt, were observed. These wide ionic domains were well connected to one another, and may provide a good ionic transporting pathway.

For fuel cell applications, water uptake (WU) and hydroxide conductivity ( $\sigma$ ) are of particular importance. An ideal design strategy for AEM would be expected to improve the conductivity and control water uptake. In this study, the water uptake was measured after immersing the membranes in water at 20 °C for 24 h, and the data are summarized in Table 1. The comb-shaped copolymers showed lower water uptake than the PPO-TMA-20 membrane, thus exhibiting lower dimensional swelling behaviour (Table 1,  $\Delta l$ , swelling ratio in in-plane direction). The number of absorbed water molecules per QA group (designated as  $\lambda$ ) was calculated. A constant number of water molecules per QA group for PPO-DMHDA- $x$  membranes was observed even at high ion exchange capacity (IEC) level (PPO-DMHDA-55, IEC = 1.92 meq. g<sup>-1</sup>,  $\lambda$  = 5.9). Unlike previously reported comb-shaped PEM,<sup>37</sup> in which the comb-shaped structure induced a high water uptake, the PPO-DMHDA- $x$  displayed much lower water uptake than PPO-TMA and other aromatic AEMs (e.g.  $\lambda > 10$ ).<sup>18–24</sup>

Impedance spectroscopy (in water under an active argon gas purge in an attempt to limit the exposure of the OH<sup>-</sup> form membranes to CO<sub>2</sub>) revealed that the comb-shaped membranes had excellent hydroxide conductivities which were in the range of 7–35 mS cm<sup>-1</sup> at 20 °C. These values were much higher than those of PPO-TMA-20 (5 S cm<sup>-1</sup>) (Table 1) under the same testing conditions. The PPO-DMHDA-55 membrane achieved the highest hydroxide conductivity of 35 S cm<sup>-1</sup> at 20 °C. In most AEMs, the hydroxide conductivities of

**Table 1** Properties of comb-shaped PPO-DMHDA- $x$  and PPO-TMA-20 membranes

Samples	IEC (meq. g <sup>-1</sup> )	WU (wt%) <sup>a</sup>	$\lambda$	$\Delta l$ (%)	$\sigma$ (mS cm <sup>-1</sup> ) <sup>a</sup>
PPO-DMHDA-20	1.08	8.2	5.6	2.6	7
PPO-DMHDA-30	1.48	13.5	5.2	4.2	14
PPO-DMHDA-40	1.67	16.2	5.4	5.0	23
PPO-DMHDA-55	1.92	20.4	5.9	5.6	35
PPO-TMA-20	1.39	25.9	10.4	7.4	5

<sup>a</sup> Measured in water at room temperature (20 °C).

the membranes are strongly related to the IEC values or the water uptake of the membrane, and AEMs absorbing a large amount of water typically have a high hydroxide conductivity.<sup>18</sup> Therefore, there is a good correlation between the IEC or water uptake and hydroxide conductivity. However, as apparent from Table 1, IEC or water uptake values of the comb-shaped membranes are lower than those of PPO-TMA, indicating that the polymer structure, such as the phase separation (as confirmed by SAXS) formed in the comb-shaped membrane, influenced the hydroxide conductivity. Compared to some of the reported AEMs,<sup>19–25</sup> our comb-shaped polymer membranes still showed higher hydroxide conductivity, as shown in Fig. 2a. As demonstrated by McGrath and co-workers, the continuity of nanoscale domains is critical to efficient proton transport in sulfonated polymers.<sup>38</sup> For our comb copolymers, the nano-phase separated structures documented above also clearly enhance hydroxide conductivity under hydrated conditions by almost three times compared with the typical AEM based on trimethylamine (PPO-TMA).

The important point is that the comb-shaped PPO-DMHDA- $x$  membranes showed a much lower water uptake but a comparable conductivity compared with the reported values for quaternary ammonium AEMs in the hydroxide form. The polysulfone AEMs with a quaternary ammonium group reported by Zhang<sup>24</sup> and co-workers exhibited a water uptake of 32% and OH<sup>-</sup> conductivity of 32 mS cm<sup>-1</sup> at 20 °C, and the quaternary phosphonium AEM reported by Yan *et al.*<sup>23</sup> had a OH<sup>-</sup> conductivity 27 mS cm<sup>-1</sup> at 20 °C. Overall, the PPO-DMHDA- $x$  membranes located at the left upper hand part of Fig. 3b indicate high hydroxide conductivity but lower water absorption ( $\lambda$  value). These results suggest that our concept to apply the comb-shaped structure is effective for the AEMs for mitigating water swelling and improving conductivity.

Recently, the rapid uptake of CO<sub>2</sub> by AEMs was confirmed by Yanagi<sup>39</sup> and Hickner,<sup>21</sup> who reported that OH<sup>-</sup> was neutralized quickly upon exposure to air because of the rapid absorption of CO<sub>2</sub>, causing a corresponding decrease in ionic conductivity due to the lower mobility of HCO<sub>3</sub><sup>-</sup> ions in dilute solution. Thus, the conductivity was measured over several tens of hours with the water exposed to atmospheric CO<sub>2</sub>. As shown in Fig. 4a, after initial ion exchange of the membrane to the hydroxide form, the conductivity of the samples steadily declined over a period of 1–20 h, which was ascribed to sorption of CO<sub>2</sub>. After 2 days of exposure of the membrane in water to ambient air, the conductivity of the samples was the same as for samples purposely ion exchanged to bicarbonate form. The OH<sup>-</sup>–HCO<sub>3</sub><sup>-</sup> conductivity ratios for the samples are reported Fig. 4b. From the dilute-solution mobilities of the anions, the OH<sup>-</sup>–HCO<sub>3</sub><sup>-</sup> conductivity ratio should be 4.4, assuming that the activities of the ions remain constant.<sup>12,13</sup> The low water uptake of comb-shaped

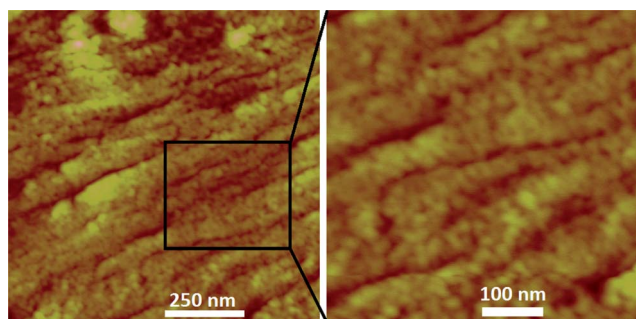


**Fig. 2** The AFM images of PPO-DMHDA-20 membrane.



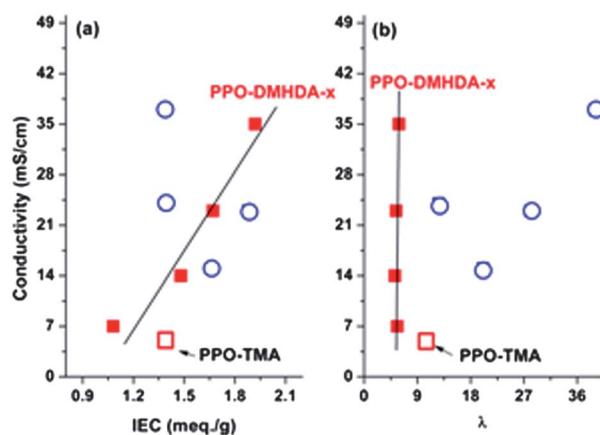


**Fig. 3** Hydroxide conductivity of PPO-DMHDA-*x* (solid square), PPO-TMA (open square), and some literature reported AEMs<sup>19,20,23,24</sup> (open circle) at 20 °C as a function of (left) ion exchange capacity (IEC) and (right) the adsorbed water molecules per QA-group ( $\lambda$  value).

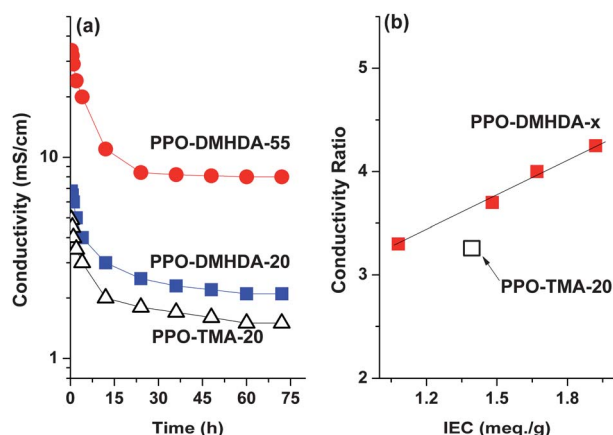


**Fig. 4** (a) Decline in conductivity of the hydroxide form AEMs during conductivity measurements open to atmosphere after 3 days; (b) the  $\text{OH}^-/\text{HCO}_3^-$  conductivity ratios for all AEMs. Conductivities were measured with samples exposed to liquid water at 20 °C.

membranes likely leads to the low conductivity ratio, while the membrane PPO-DMHDA-55 with high water uptake had a high ratio of 4.3. Furthermore, the  $\text{HCO}_3^-$  conductivity increased linearly with temperature for all five AEMs when they were fully hydrated, as shown in Fig. S5†. The PPO-DMHDA-55 membrane (IEC = 1.92 meq. g<sup>-1</sup>) showed the highest conductivity of 19 mS cm<sup>-1</sup> at 80 °C, which is comparable to the values reported for quaternary ammonium AEMs in the  $\text{HCO}_3^-$  form (10.1–25.7 mS cm<sup>-1</sup>).<sup>21,40</sup>

To further explore the reliability of the comb-shaped polymers, we monitored the stability at 80 °C in 1 M NaOH aqueous solution. The PPO-TMA-20 membrane was broken into small pieces after 80 h stability testing. Its hydroxide conductivity decreased rapidly to 2.1 mS cm<sup>-1</sup>, which was ~40% of the initial value (Fig. 5a). After an initial period of transient behavior for several tens of hours, the IEC of PPO-TMA-20 showed a constant but slow decline starting from 0.95 meq. g<sup>-1</sup>, as shown in Fig. 4b. However, the comb-shaped PPO-DMHDA-20 and PPO-DMHDA-40 membranes maintained their toughness, flexibility, and appearance after 500 h. The hydroxide conductivity of PPO-DMHDA-40 after the test of 500 h was

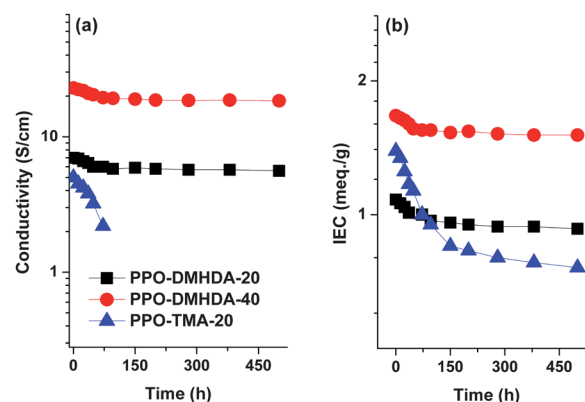


**Fig. 5** The changing trend in (a) hydroxide conductivity and (b) IEC values of comb-shaped and PPO-TMA membranes after immersion in 1 M NaOH solution at 80 °C.

estimated to be 18.5 mS cm<sup>-1</sup>, which was ~80% of the initial hydroxide conductivity value of 23 mS cm<sup>-1</sup> (Fig. 5a), suggesting the comb-shaped membranes have better alkaline stability than the non-comb-shaped membrane PPO-TMA, and have sufficient long-term stability for AEM fuel cell application. As shown in Fig. 5b, the IEC value of comb-shaped copolymer membranes changed little during the stability testing, which further confirms the improved alkaline stability of comb-shaped AEMs.

It has already been demonstrated that the quaternary ammonium groups have a tendency to disintegrate in alkaline solution at high temperature due to the displacement of the ammonium group by  $\text{OH}^-$  via a direct nucleophilic substitution and/or Hofmann elimination when  $\beta$ -hydrogen atoms are present.<sup>18</sup> In the present study, there are two  $\beta$ -hydrogen atoms around the quaternary ammonium groups in comb-shaped membranes, and the Hofmann elimination reaction could occur. Therefore, the degradation of comb-shaped membranes is due to both direct nucleophilic substitution and Hofmann elimination while the PPO-TMA without  $\beta$ -hydrogen was degraded mainly by the nucleophilic substitution in which the hydroxides attack the  $\alpha$ -carbon of ammonium cations. Although the Hofmann elimination is the preferred decomposition pathway for ammonium cations bearing  $\beta$ -hydrogens which has been proved by Pivovar *et al.* using density functional theory (DFT) calculation,<sup>41,42</sup> the comb-shaped membranes displayed better alkaline stability than PPO-TMA without  $\beta$ -hydrogen. The excellent alkaline stability presumably results from the presence of large volumetric  $\beta$ -alkyl chains, which may hinder Hofmann elimination and protect the ammonium cations from being attacked by  $\text{OH}^-$ , or from the fact that only two rather than three  $\beta$ -hydrogen sites exist for Hofmann elimination.<sup>41,42</sup>

In summary, we have designed, synthesized and characterized a new class of comb-shaped polymers for anion exchange membranes. The comb-shaped polymer exhibits nanoscale-organized phase separated morphology, resulting in an enhancement in conductivity relative to the typically hydrocarbon-based AEMs aminated by trimethylamine. These results suggest that our concept of applying the comb-shaped structure is effective for the AEMs in mitigating water swelling and improving hydroxide conductivity. The combination of excellent solubility in some low-boiling-point water-soluble solvents and outstanding alkaline stability makes comb-shaped membranes attractive as AEM materials for fuel cell

applications. Further investigations on this class of comb-shaped AEM materials are ongoing in our laboratory. Future work will focus on studying their efficacy under operating conditions and investigating AEMs with different lengths of grafting chain polymer backbones.

## Acknowledgements

Nanwen Li thanks the Alexander von Humboldt Foundation for financial support.

## Notes and references

- 1 R. J. P. Williams, *Annu. Rev. Biophys. Biophys. Chem.*, 1988, **17**, 71–97.
- 2 K. D. Kreuer, *Chem. Mater.*, 1996, **8**, 610–641.
- 3 T. Sata, *Pure Appl. Chem.*, 1986, **58**, 1613–1626.
- 4 C. H. Park, C. H. Lee, M. D. Guiver and Y. M. Lee, *Prog. Polym. Sci.*, 2011, **36**, 1443–1498.
- 5 N. P. Brandon, S. Skinner and B. C. H. Steele, *Annu. Rev. Mater. Res.*, 2003, **33**, 183–213.
- 6 M. A. Hickner, H. Ghassemi, Y. S. Kim, B. R. Einsla and G. E. McGrath, *Chem. Rev.*, 2004, **104**, 4587–4611.
- 7 T. Xu, *J. Membr. Sci.*, 2005, **263**, 1–29.
- 8 G. F. McLean, T. Niet, S. Prince-Richard and N. Djilali, *Int. J. Hydrogen Energy*, 2002, **27**, 507–526.
- 9 P. K. Shen, C. Xu, H. Meng and R. Zeng, *Adv. Fuel Cells*, 2005, 149–179.
- 10 G. Merle, M. Wessling and K. Nijmeijer, *J. Membr. Sci.*, 2011, **377**, 1–35.
- 11 J. S. Spendelow and A. Wieckowski, *Phys. Chem. Chem. Phys.*, 2007, **9**, 2654–2675.
- 12 J. A. Dean, *Lange's Handbook of Chemistry*, McGraw-Hill, New York, 15th edn, 1999.
- 13 P. Vanysek, Ionic Conductivity and Diffusion at Infinite Dilution, in *CRC Handbook of Chemistry and Physics*, ed. D. R. Lide, CRC Press, Boca Raton, 83rd edn, 2002.
- 14 S. T. Milner, *Macromolecules*, 1994, **27**, 2333–2335.
- 15 E. M. W. Tsang, Z. B. Zhang, Z. Q. Shi, T. Soboleva and S. Holdcroft, *J. Am. Chem. Soc.*, 2007, **129**, 15106–15107.
- 16 Z. C. Zhang, E. Chalkova, M. Fedkin, C. Wang, S. N. Lvov, S. Komarneni and T. C. Chung, *Macromolecules*, 2008, **41**, 9130–9139.
- 17 K. D. Kreuer, *J. Membr. Sci.*, 2001, **185**, 29–39.
- 18 J. R. Varcoe and R. C. T. Slade, *Fuel Cells*, 2005, **5**, 187–200.
- 19 M. R. Hibbs, C. H. Fujimoto and C. J. Cornelius, *Macromolecules*, 2009, **42**, 8316–8321.
- 20 J. R. Varcoe, R. T. C. Slade, E. L. H. Yee, S. D. Poynton, D. J. Driscoll and D. C. Apperley, *Chem. Mater.*, 2007, **19**, 2686–2693.
- 21 J. Yan and M. A. Hickner, *Macromolecules*, 2010, **43**, 2349–2356.
- 22 M. R. Hibbs, M. A. Hickner, T. M. Alam, S. K. McIntyre, C. H. Fujimoto and C. J. Cornelius, *Chem. Mater.*, 2008, **20**, 2566–2573.
- 23 S. Gu, R. Cai, T. Luo, Z. Chen, M. Sun, Y. Liu, G. He and Y. Yan, *Angew. Chem., Int. Ed.*, 2009, **48**, 6499–6502.
- 24 J. H. Wang, Z. Zhao, F. X. Gong, S. H. Li and S. B. Zhang, *Macromolecules*, 2009, **42**, 8711–8717.
- 25 J. H. Wang, S. H. Li and S. B. Zhang, *Macromolecules*, 2010, **43**, 3890–3896.
- 26 J. S. Park, S. H. Park, S. D. Yim, Y. G. Yoon, W. Y. Lee and C. S. Kim, *J. Power Sources*, 2008, **178**, 620–626.
- 27 J. S. Park, G. G. Park, S. H. Park, Y. G. Yoon, C. S. Kim and W. Y. Lee, *Macromol. Symp.*, 2007, **249–250**, 174–182.
- 28 Z. Zhao, J. H. Wang, S. H. Li and S. B. Zhang, *J. Power Sources*, 2011, **196**, 4445–4450.
- 29 M. Tanaka, K. Fukasawa, E. Nishino, S. Yamaguchi, K. Yamada, H. Tanaka, B. Bae, K. Miyatake and M. Watanabe, *J. Am. Chem. Soc.*, 2011, **133**, 10646–10654.
- 30 Y. Yang and S. Holdcroft, *Fuel Cells*, 2005, **5**, 171–186.
- 31 T. Xu, D. Wu and L. Wu, *Prog. Polym. Sci.*, 2008, **33**, 894–915.
- 32 T. Xu and W. Yang, *J. Membr. Sci.*, 2001, **190**, 159–166.
- 33 S. Zhang, T. Xu and C. Wu, *J. Membr. Sci.*, 2006, **269**, 142–151.
- 34 K. Nakamura and K. Fukao, *Macromolecules*, 2011, **44**, 3053–3061.
- 35 M. Beiner and H. Huth, *Nat. Mater.*, 2003, **2**, 595–599.
- 36 M. Antonietti, J. Conrad and A. Thunemann, *Macromolecules*, 1994, **27**, 6007–6011.
- 37 N. Li, C. Wang, S. Y. Lee, C. H. Park, Y. M. Lee and M. D. Guiver, *Angew. Chem., Int. Ed.*, 2011, **50**, 9158–9161.
- 38 A. Roy, M. A. Hickner, X. Yu, Y. Li, T. E. Glass and J. E. McGrath, *J. Polym. Sci., Part B: Polym. Phys.*, 2006, **44**, 2226–2239.
- 39 H. Yanagi and K. Fukuta, *ECS Trans.*, 2008, **16**, 257–262.
- 40 N. J. Robertson, H. A. Kostalik, T. J. Clark, P. F. Mutolo, H. D. Abruna and G. W. Coates, *J. Am. Chem. Soc.*, 2010, **132**, 3400–3404.
- 41 B. E. Joseph, C. S. Macomber, B. S. Pivovar and J. M. Boncella, *J. Membr. Sci.*, 2012, **399–400**, 49–59.
- 42 H. Long, K. Kim and B. S. Pivovar, *J. Phys. Chem. C*, 2012, **116**, 9419–9426.